Interaction of Oxygen Carriers with Common Biomass Ash Components

Ivana Staničić[1*], Malin Hanning[1], Robin Deniz[2], Tobias Mattisson[1], Rainer Backman[3], Henrik Leion[2]

[1] Department of Space, Earth and Environment, Division of Energy Technology, Chalmers University of Technology, SE-412 96 Gothenburg, Sweden

[2]Department of Chemistry and Chemical Engineering, Chalmers University of Technology, SE-412 96 Gothenburg, Sweden

[3] Department of Applied Physics and Electronics, Thermochemical Energy Conversion Laboratory, Umeå University, SE 901 87 Umeå, Sweden

[*]stanicic@chalmers.se

Abstract

Carbon capture and storage (CCS) has been proposed as a bridging technology between the current energy production and a future renewable energy system. One promising carbon capture technology is chemical-looping combustion (CLC). In CLC the reactors are filled with metal oxide bed material called oxygen carriers. The interaction between oxygen carriers and biomass ashes is a poorly explored field. To make CLC a viable process, and thereby creating carbon emission reductions, more knowledge about the interactions between biomass ashes and oxygen carriers is needed.

This study investigated solid-state reactions of three promising oxygen carriers, hematite, hausmannite and synthesised ilmenite with different biomass ash components. Oxygen carriers were exposed with the ash components: calcium carbonate, silica and potassium carbonate at 900°C and at different reducing potentials. Crystalline phases of the exposed samples were determined using powder x-ray diffraction (XRD).

Results showed that the oxygen carriers hausmannite and hematite interact to a higher extent compared to synthesised ilmenite regarding both physical characteristics and detectable phases. Synthesised ilmenite formed new phases only in systems including potassium.

Thermodynamic calculations were performed on the multicomponent system and compared with experimental results. The results suggest that optimisation of systems involving manganese and potassium should be performed.

Keywords: Oxygen carrier; Biomass ash; Chemical Looping Combustion (CLC); Ilmenite

1. Introduction

The concentrations of greenhouse gases in the atmosphere are increasing as the result of anthropologic activities, where the extensive combustion of fossil fuels is the main reason for the increase. A quarter of the total emissions of greenhouse gases originate from the production of electricity and heat, where the main energy source is fossil fuels [1, 2].The increasing global mean temperature, with subsequent climate change, are the severe consequences of these activities. In fact, a recent report from the UN indicates that it is almost impossible for the world to meet the limits set in the Paris agreement, as the carbon budget for limited warming is almost exhausted [3]. This means that it may be necessary to remove carbon dioxide from the atmosphere in order to limit warming.

Carbon capture and storage (CCS) has been proposed as a bridging technology between the current energy production and a future renewable energy system. The CCS concept consists of the capture of carbon dioxide from point sources such as power plants, followed by compression, transportation and finally deposition at a storage site [4]. Bioenergy with carbon capture and storage (BECCS) could even make it possible to achieve negative greenhouse gas emissions, which is now necessary if the climate targets are to be reached [5, 6].

Chemical-looping combustion (CLC) is one technology proposed for capturing carbon dioxide from combustion facilities [7]. It is based on the use of metal oxides with the ability to be oxidised or reduced at combustion conditions depending on the surrounding oxygen partial pressure [8]. Thus, the need for gas separation can be avoided, and carbon dioxide may be captured at a much lower cost than with other technologies [9]. Numerous metal oxides, referred to as oxygen carriers, have been operated in chemical-looping units ranging from small lab-scale units up to a 1 MW_{th} reactor [10]. The use of biomass in CLC is increasing, which can clearly be seen in the recent review article by Adánez et al [11]. For example, a 1 MW_{th} chemical-looping pilot plant has been operated with a fuel mix of hard coal and torrefied biomass [12]. The manganese ore examined in this paper has also been used as oxygen carrier in two pilot scaled chemical-looping pilots, 10 kW_{th} and 100 kW_{th}, with wood char and pellets as fuels [13]. To make CLC a viable process for BECCS, more knowledge about the interactions between biomass ashes and oxygen carriers is needed, as it is well known that biomass ash can be aggressive and corrosive during thermal conversion at high temperature.

In addition to CLC, there are other technologies utilizing oxygen carriers for fuel conversion. For example, the use of oxygen carriers in conventional combustion in fluidised bed boilers has been proposed as a measure to even out the oxygen availability and temperature in the boiler. This technology has been referred to as oxygen carrier aided combustion (OCAC) and promising results have been reported [14-16]. The concept has been successfully operated for more than 12,000 h using ilmenite as bed material in full industrial scale [17]. OCAC is currently being commercialized [17].

In any technology utilizing oxygen carriers with biomass, one important issue is whether ash components in the fuel will interact with the oxygen carrier and how this will affect the performance of the system. Consequences of interactions between conventional bed materials in fluidized beds and biomass ashes have been widely studied [18-21]. A few studies have been made concerning biomass ash interaction with the oxygen carriers ilmenite, iron ore and manganese ore [15, 22, 23]. This is however still a poorly explored field of research.

The objective of this study is to systematically investigate interactions between three commonly used oxygen carriers and three biomass ash components containing calcium, silicon and potassium respectively, all elements known for interacting with bed materials during combustion.

2. Background

2.1. Chemical-Looping Combustion and Oxygen Carrier Aided Combustion

In chemical-looping combustion (CLC), the oxygen carrier will change oxidation state depending upon the surrounding chemical environment and temperature. In this way, combustion can be carried out in two separate reactor vessels without gas mixing between the two. The metal oxide is oxidised by air in one vessel, the air reactor (AR), and reduced by the fuel in the other, the fuel reactor (FR). The fuel is thus oxidised in the fuel reactor by the solid-state oxygen supplied by the oxygen carrier. A simplified scheme of this combustion concept is illustrated in Figure 1.

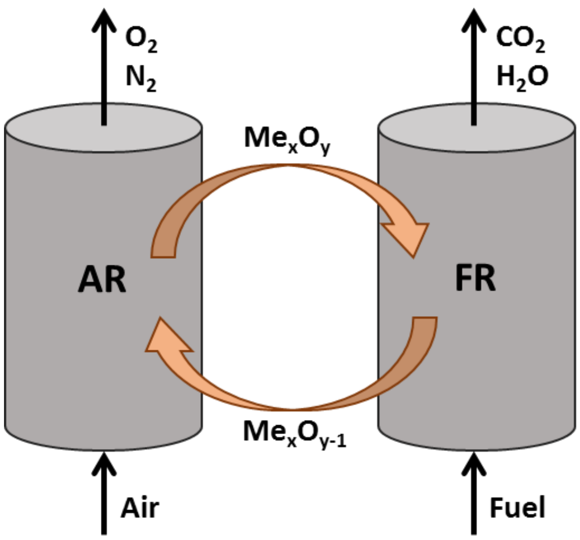

Figure 1 The combustion scheme of chemical-looping combustion.

The heat of combustion will be identical to normal combustion in air. This can be shown by adding up the two overall reaction steps shown below, where reaction 1 occurs in the air reactor and reaction 2 in the fuel reactor:

$$Me_xO_{y-1} + \frac{1}{2}O_2 \rightarrow Me_xO_y \quad (1)$$

$$(2n+m)Me_xO_y + C_nH_{2m} \rightarrow (2n+m)Me_xO_{y-1} + mH_2O + nCO_2 \quad (2)$$

A common way to realise chemical-looping combustion is by using two interconnected fluidised bed reactors. The oxygen carrier has the form of small particles of a suitable size range. By using this method, knowledge and experience of combustion in circulating fluidised bed (CFB) boilers can be used. The air reactor is a circulating fluidised bed with high gas velocities, which is needed to transport the particles from the bed to the fuel reactor. The fuel reactor can either be a bubbling bed with lower gas velocities or a circulating fluidised bed with an internal circulation loop. The latter is usually regarded to be more advantageous for solid fuels, due to mixing issues and possibilities for scale-up. Most chemical-looping pilot units in operation today use interconnected fluidised beds as combustion method [24].

When oxygen carriers are used in conventional fluidised bed combustion (OCAC) the oxygen carrier transport oxygen in the same way as in CLC, i.e. by reaction 1 and 2. But instead of an oxidizing and reducing reactor the oxygen transport is between oxygen rich and oxygen depleted zones in a single reactor, the combustion chamber. This evens out temperature gradients reducing the risk of hotspots which in general gives smoother operation of the boiler.

2.2. Oxygen Carriers

As is seen in reactions 1 and 2 above, the metal oxide is in most cases not reduced fully to the metallic state, although this is a possibility and depends on the metal oxide used. The combustion route will differ depending on the type of fuel being burnt. Gaseous fuels can react directly with the oxygen carrier in a gas-solid reaction. In CLC with a solid fuel, the volatiles will first be released in gaseous form and then react directly with the oxygen carrier. The remaining char needs to be gasified by H_2O or CO_2 present in the fuel reactor, to CO and H_2, which can react with the oxygen carrier in a gas-solid reaction.

In CLC, char gasification with steam is rather slow compared to the other reactions in the combustion scheme and would therefore be the rate limiting factor for the conversion of the fuel. This could be problematic, as a long fuel residence time in the fuel reactor may be needed for complete burnout. However, some metal oxides are capable of releasing oxygen in gaseous form at temperatures relevant for fuel combustion and the char can then react directly with the gaseous oxygen released and will not need to be gasified. This combustion scheme is referred to as chemical-looping with oxygen uncoupling (CLOU) [25].

There are several properties needed for materials to be suitable as oxygen carriers including high reaction rates and resistance towards chemical and mechanical stress. The material should not be deactivated by fuel impurities such as sulphur or ash components. At commercial scale, large quantities of the oxygen carrier material will need to be handled. Therefore, it is preferable if the material is rather cheap and neither toxic nor environmentally harmful.

Iron-based oxygen carriers are both environmentally friendly and relatively cheap due to their abundance [26]. Furthermore, iron-based oxygen carriers have high melting temperatures which reduces the risk of agglomerations [27]. Iron oxides can be oxidised and reduced between several oxidation states: Fe_2O_3/Fe_3O_4, Fe_3O_4/FeO and FeO/Fe. A study by Jerndal et al. [27] showed that Fe_2O_3/Fe_3O_4 should be most favourable for conditions used in a CLC process. A major disadvantage using iron-based oxygen carriers is that they show comparably low oxygen transport capacity [28]. There are various iron ores that have shown favourable attributes as oxygen carriers and have been operated in CLC pilots [29, 30]. Ilmenite is an iron and titanium ore, which has been extensively examined as oxygen carrier [31-34]. Ilmenite has good fluidisation properties, high melting point, low production of fines and can be utilised without much pre-treatment as an oxygen carrier. It has also been used as an oxygen carrier in several commercial CHP units in Sweden, based on fluidized bed combustion and oxygen carrier aided combustion [17]. A recent review article has summarised the research on iron oxygen carriers [35].

Manganese-based oxygen carriers are non-toxic, relatively cheap and have a high melting temperature. Out of the manganese systems Mn_2O_3/Mn_3O_4, Mn_3O_4/MnO and MnO/Mn, only Mn_3O_4/MnO is feasible for conditions used in a high temperature CLC process [27]. A manganese oxygen carrier was operated in a reactor system designed for a thermal power of 300 W for 70 h with natural gas and syngas as fuels. No tendencies of agglomeration or deactivation of the oxygen carrier was detected [36]. Manganese ores have been examined during continuous operation with both gaseous [37, 38] and solid fuels [39-41] with promising results. A study by Arjmand et al. [42] showed that manganese ores has attributes feasible for CLOU, but that the impurities in the ores contributed to these properties.

2.3. Interactions between Biomass Ash and Oxygen Carriers

The amount and composition of ash varies widely depending on the type of biomass used as fuel [43]. The ash contains inorganic matter that remains after the fuel is combusted. The most common elements in biomass ash are calcium, potassium, silicon, magnesium, aluminium, sulphur, iron, phosphorous, chlorine, sodium and trace elements [44]. Depending on the composition and physical state of the ash, ash-related problems could occur. such as fouling, slagging, corrosion and bed agglomeration [45, 46]. Agglomeration is described by Zevenhoven et al. [45] as the phenomenon where particles gather into clusters of larger size than the original particles and could cause de-fluidisation of a bed. Even though physical phenomena play a role, formation of coatings is usually a prerequisite for agglomeration. Coatings on bed material could form in different ways. For instance, the coating can be independent of the bed material which act as an inert material. In this case the coating can grow outwards incorporating elements released from the fuel. The coating could also grow inwards, where only the reactive elements will interact with the bed particle. Coating formation could also take place by reaction between silicon, calcium and potassium. However, in practice these three elements will most likely not coincide [45]. Silicon could react with calcium to form calcium silicates, which has a melting point above 1500°C. This compound could then stick to the bed material surface. Another mechanism described by Zevenhoven et al. [45] is more likely since bed agglomeration is usually observed around 800°C. Silicon may react with gaseous potassium to form potassium silicate which has a melting point around 750°C. If calcium components are incorporated into this layer the melting point may be raised to 800°C. This sticky compound could then form a layer on the bed material. Additionally, if a molten phase is present two particles could be glued together. If there are enough molten ash particles present, agglomerates could form which in its turn could lead to de-fluidisation of the bed.

The characterisation of ash components and the ash transformation processes are important for the operation of a fluidised bed boiler. Potassium is most often the main alkali source in biomass ashes and is an especially problematic ash component. Potassium commonly reacts with chlorine and forms gaseous potassium chloride in fuels with high content of Cl. This compound is a cause of corrosion and fouling in the convection path of the boiler. The formation of alkali chloride compounds also promotes the reaction of the alkali with silicates since the mobility of alkali increases when present in gaseous form [47, 48]. When potassium reacts with silica sand, the most common bed material in fluidised bed boilers, sticky ash compounds are formed on the surface of particles. This leads to particles merging together to larger clusters forming agglomerates [19].

Ash interactions with an oxygen carrier could cause additional effects apart from agglomeration. Ash components attaching to the surface of the particles may affect the oxidation and reduction rates of the oxygen carrier. The reaction rate can be reduced if gas diffusion is hindered by an ash layer formed on the surface of particles. On the other hand, attached ash components could potentially have catalysing effects on different reactions, or even have oxygen carrier properties in themselves, which may be an advantage. Ash components reacting with the oxygen carrier and forming new compounds could either increase or decrease the oxygen transport capacity. It is also important to consider that the gaseous environment in the fuel reactor of a CLC, where the fuel is converted, differs from a normal combustion chamber, as there is very little free oxygen, and hence a higher degree of reduction. This could result in a different ash transformation process, compared to normal combustion.

The research on interactions between ash and oxygen carriers has so far mainly been focused on coal ashes. Studies on coal fly ash and oxygen carriers have shown no or very limited interaction [49, 50]. Wang et al. [51], on the other hand, reported the formation of iron silicates when cycling a copper-iron oxygen carrier with hydrogen as fuel. Azis et al. [52] concluded that a small addition of coal ash to ilmenite reduced the reactivity of the oxygen carrier, but further addition of ash substantially increased the gas conversion. Similar contradictory results have been reported for lignite ash with an iron oxygen carrier [53]. Keller et al. [54] concluded that the mineral pyrite had the most deteriorating effect on the oxygen carrier reactivity due to formation of sulphides, when studying interactions between minerals commonly found in ashes and oxygen carriers, including ilmenite. It was, however, shown that ilmenite did not form any sulphides [54]. Bao et al. [55] investigated the effect of common coal ash components on iron oxygen carriers and found that most of the ash components decreased the reactivity, except calcium sulphate which can function as an oxygen carrier itself. Calcium can also increase the rate of the water-gas-shift reaction which indirectly gives an improved fuel conversion [56]. A recent study showed that brown coal ash, which is rich in silica, iron and magnesium, reacted both with iron ore and with ilmenite [57]. Gong et al. [58] found that the solid conversion during oxygen uncoupling was lowered when a copper oxygen carrier was mixed with coal ashes.

There are a limited number of studies on interactions between biomass ash and oxygen carriers in CLC. Zhang, S. and Xiao, R. used laboratory fluidised bed systems to evaluate ash modified and unmodified iron ores [59]. Iron ores were modified using lignite coal ash and three different biomass ashes (wheat stalk ash, corn stalk ash and soybean stalk ash). These ashes contained different relative amounts of K_2O, CaO and Na_2O. The study identified interaction between potassium and iron and formation of the following compounds; $K_2Fe_4O_7$, $K_2Fe_{10}O_{16}$, $K_2Fe_{22}O_{34}$, and $K_{1.11}Fe_{1.11}Si_{0.89}O_4$. Calcium on the other hand was found to have difficulties interacting with iron [59]. Gu et al. [23] concluded that ash rich in silica caused sintering and agglomeration of an iron ore, while potassium-rich ash increased the reduction reactivity of the ore. Corcoran et al. [60] examined ilmenite as oxygen-carrying bed material for OCAC. When studying ilmenite particles that had been operated in a 12 MW_{th} CFB boiler with biomass as fuel, it was seen that a segregation of iron to the surfaces and an enrichment of titanium in the particle core had taken place. A calcium-rich double layer on the particle had also been formed, which surrounded the iron layer [60]. Both the separation of titanium and iron as well as the calcium layer have been observed previously in CLC conditions [52]. Other studies have found that with increased time of exposure, potassium migrates into the ilmenite particle core [22], and that depending on the chemical compound of potassium when interacting with ilmenite will lead to different outcomes [61].

3. Materials and Methods

3.1. Oxygen Carriers and Ash Components

Three common oxygen carriers were chosen for investigation: hematite (Fe_2O_3), hausmannite (Mn_3O_4) and synthesised ilmenite ($FeTiO_3$). Their composition and properties are summarised in *Table 1*. The hematite and hausmannite have previously been studied by Leion et al under the name of *Höganas* and *Colormax S* respectively [62]. Hematite and hausmannite are monometallic systems and they were early on proposed as oxygen carriers. Ilmenite is an iron and titanium ore commonly used as oxygen carrier. In this case synthesised particles were used to avoid affecting the results by impurities common in naturally occurring materials. This synthesised ilmenite was produced by freeze granulation [63], details of the production methods can be found elsewhere [64].

Table 1. Composition and properties of the oxygen carriers studied.

Oxygen carrier	Composition	Oxidised/reduced form	Particle size (µm)	Previous work
Hematite	84.0% Fe_2O_3 16.0% Fe_3O_4	Fe_2O_3/Fe_3O_4	125-180	[62]
Hausmannite	93.7% Mn_3O_4 6.3% MnO	Mn_3O_4/MnO	125-180	[62]
Synthesised ilmenite	87.6% Fe_2TiO_5 12.4% TiO_2	$Fe_2TiO_5 + TiO_2/FeTiO_3$	125-180	[63]

The three most common elements of biomass ash were used to study their interactions with the oxygen carriers selected: calcium, potassium, and silicon [44]. The oxygen carrier and ash components were mixed and exposed to high temperature and different atmospheres. Calcium and potassium were added as carbonates, forming oxides and carbon dioxide during heat-up. Silica was used as it is a common silicon compound found in ashes. The details of the ash components can be found in Table 2.

Table 2. Composition and properties of the ash components used.

Ash component	Composition	Particle size (µm)	Origin
Calcium carbonate	≥99% $CaCO_3$	100-315 µm	Merck
Potassium carbonate	≥99% K_2CO_3	44 µm	Sigma-Aldrich
Silicon dioxide	≥99% SiO_2	<30 µm	Sigma-Aldrich

3.2. Experimental Setup and Procedure

The oxygen carriers and ash components were exposed to oxidising and reducing conditions in fixed-bed tubular furnaces together with tubular quartz reactors as presented in *Figure 2*. Both furnaces were manufactured by Vecstar, model VCTF4. Air was used for the oxidising conditions and 2.5% H_2, 47.5% Ar and 50% H_2O were used for the reducing conditions, which may correspond reasonably well with the reducing potential which is present in a fuel reactor of a chemical-looping combustor. The reducing potential, pH_2/pH_2O is 0.05 which corresponds to an equilibrium partial pressure of O_2 of $\log_{10}p(O_2)$ of -13.7 atm. Further, the high concentration of H_2O means that the lowest forms of iron oxide i.e. FeO, will not form from a thermodynamic point of view. The total flow through the reactors was 140 Nml/min. The air flow was controlled by a needle valve and the steam flow by a water pump (Watson Marlow 120U). A rotameter controlled the nitrogen and hydrogen in argon flow.

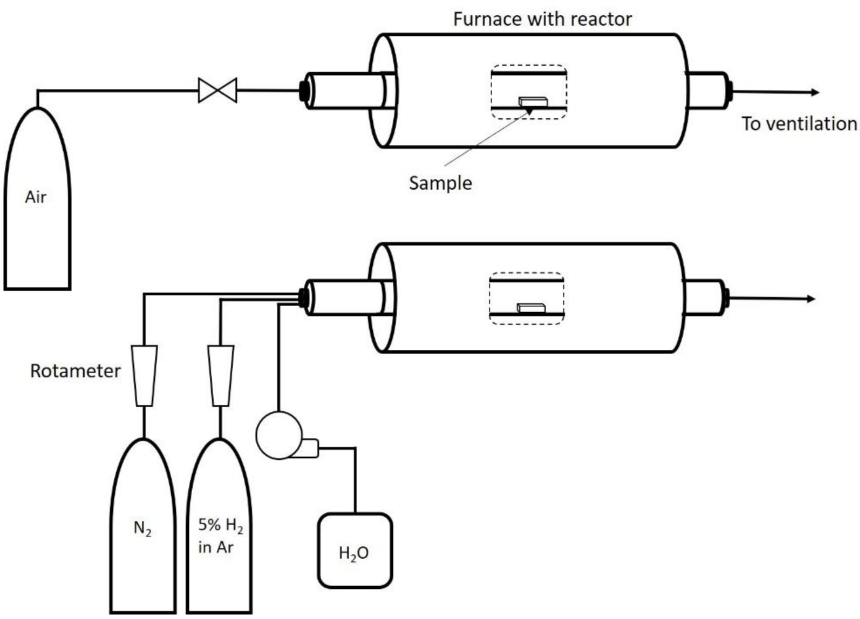

Figure 2 Schematic overview of the experimental system [65].

All experiments were performed at atmospheric pressure. Before the exposures, the temperature profiles of the furnaces were determined with a thermocouple to know the exact position for the measured temperature. The furnace was heated to 900°C and the holding time was 6 h before the furnace was cooled down. Six hours holding time was chosen, as it was judged to be sufficient to achieve some interactions between the compounds at these temperatures, although it cannot be established if thermodynamic equilibrium was reached. Still, if the content after exposure has not reached thermodynamic equilibrium it is not expected to be reached in a fluidised bed setup either. This experimental setup with long exposure time and enhanced contact allows one to investigate reaction possibilities in certain important systems. When reducing conditions were used, the heat-up and the cool-down were carried out in an inert atmosphere of nitrogen. The same experimental setup has been previously used to study ash interactions with manganese-based oxygen carriers [65].

The total sample weight was 5 g and the molar ratio of oxygen carrier and ash component was 1:1 or 1:0.5:0.5 when two ash components were used. The exposures were done according to the plan presented in Table 3. Here it is clear that each oxygen carrier was exposed to either one or two ash components for each test. When referring to the different systems the terms *binary* and *ternary* will be used. Binary systems refer to systems containing one oxygen carrier and one ash component, while ternary systems refer to one with one oxygen carrier and two ash components.

Table 3. Combinations of oxygen carrier and ash components used in the exposures.

Oxygen Carrier \ Ash component	$CaCO_3$	K_2CO_3	SiO_2
Hematite	X		
		X	
			X
	X		X
		X	X
Hausmannite	X		
		X	
			X
	X		X
		X	X
Synthesised ilmenite	X		
		X	
			X
	X		X
		X	X

3.3. Analysis Methods

After exposure and cool-down changes in sample colour and texture were noted. Visual changes were documented by photographing samples against a white background. Crystalline phases were determined using powder x-ray diffraction (XRD) with $CuK_{\alpha1}$ radiation in a Bruker D8 Advanced system. Samples were crushed in a mortar before analysed. Phases were identified using powder diffraction file (PDF) databases provided by International Centre for Diffraction Data (ICDD). These reference patterns are used to recognize chemical phases measured and each phase has a unique PDF-number.

Thermodynamic calculations were performed in FactSage 7.2®. This is an integrated database computing system. It consists of calculation and manipulation modules that can access many different solution databases and substances. FactSage 7.2® databases have been developed by optimising literature data. The program includes modules which allows calculations of conditions for multiphase, multicomponent equilibrium and phase diagrams. The module *Equilib* was used for the thermodynamic equilibrium calculations in this study. The module requires inputs of reactants and conditions such as temperature and total pressure. Possible product phases and solution databases also need to be specified. Thereafter Gibbs energy minimisation principle is used to calculate the amount of each product at chemical equilibrium state.

The molar ratio of oxygen carrier and ash component was 1:1 for binary and 1:0.5:0.5 for ternary systems. The composition of the gaseous phase is the same as that flowing through the tubular reactor. The gaseous components were introduced in large excess in the calculation, hence maintaining a relatively constant partial pressure of oxygen around the particles. Two different databases are included in this study. The databases FactPS for pure solids and FToxid for all pure oxides and oxide solutions were used. All solution phases were included in the calculations. As the ash components are heated to 900°C calculations show that they will form CaO, K_2O and SiO_2. Thus, it is not expected that carbon will be present after exposure.

4. Results

Results have been summarised in three tables below, one for each oxygen carrier. The tables contain information for each ash component and environment. The main compounds found by FactSage are presented for each exposure, in order of decreasing concentration. Compounds which are formed below 10^{-5} moles are excluded and solid (s), solid solution (ss) and slag (slag) phases are included. A solid solution is formed when a mixture of two or more crystalline solids coexist as a new crystalline solid or crystalline lattice. Each solid solution is indicated in the table with a number i.e. ss1, ss2... Ash components forming gaseous compound are also indicated in the table as (g).

Interaction between ash and oxygen carrier is indicated using italic and bold text. All samples were visually inspected before and after exposures. These observations are also described in the tables.

4.1. Hematite

Table 4 presents thermodynamic calculations together with XRD results for hematite and ash experiments. In addition, the last column provides some information regarding the visual appearance of the product.

Table 4 Summarised results for exposures carried out with hematite.

Ash component		XRD		FactSage		Visual
		Compound	**PDF No**			
$CaCO_3$	Oxidising	CaO Fe_2O_3 ***$Ca_2Fe_2O_5$***	00-037-1497 04-006-6579 00-047-1744	***$Ca_2Fe_2O_5$*** ***$CaFe_2O_4$***	(s) (s)	Soft, grey cake with pale yellow spots
	Reducing	CaO Fe_3O_4 ***$Ca_2Fe_2O_5$***	01-070-4068 04-007-1061 00-047-1744	***$Ca_2Fe_2O_5$*** Fe_3O_4	(s) (ss1)	Soft, brown and yellow cake
K_2CO_3	Oxidising	***$KFeO_2$***	04-013-8446	K_2O_2 Fe_2O_3 K KO	(s) (s) (g) (g)	Porous rock-hard black cake. Green traces.
	Reducing	***$KFeO_2$***	04-013-8446	KOH	(g) (ss1) (g)	Porous rock-hard black

				Fe_3O_4 $(KOH)_2$ K	(g)	cake. Green traces.
SiO_2	Oxidising	Fe_2O_3 SiO_2	04-006-6579 00-046-1045	Fe_2O_3 SiO_2	(s) (s)	Bright
	Reducing	Fe_3O_4 SiO_2	04-007-1061 00-046-1045	Fe_3O_4 SiO_2	(s) (s)	Darker
$CaCO_3$ and SiO_2	Oxidising	SiO_2 CaO Fe_2O_3 ***$Ca_2Fe_2O_5$***	00-046-1045 00-037-1497 01-087-1165 00-038-0408	SiO_2 Fe_2O_3 ***$Ca_3Fe_2Si_3O_{12}$***	(s) (s) (s)	Soft grey cake with pale yellow spots
	Reducing	SiO_2 CaO Fe_3O_4 ***$Ca_2Fe_2O_5$***	00-046-1045 00-037-1497 04-005-4319 00-047-1744	$CaSiO_3$ ***Fe_2SiO_4*** Fe_3O_4 ***$FeSiO_3$*** ***$CaFeSiO_4$*** ***$FeCaSiO_4$*** Ca_2SiO_4	(ss1) (ss2) (ss3) (ss1) (ss2) (ss2) (ss2)	Soft, powder. Brown and yellow cake
K_2CO_3 and SiO_2	Oxidising	***K_3FeO_4*** ***$K_{1.55}Fe_{10.92}O_{17}$*** ***$KFeO_2$*** SiO_2 Fe_2O_3	04-010-7058 04-010-3201 04-013-8446 01-071-0261 00-058-0266	Fe_2O_3 SiO_2 $K_2Si_2O_5$ K_2O	(s) (slag) (s) (slag)	Porous rock-hard black cake. Yellow spots inside with some green tones.
	Reducing	***$Fe_{2.57}Si_{0.43}O_4$*** SiO_2 K_2CO_3 Fe_3O_4 ***$Fe_{2.45}Si_{0.55}O_4$***	04-013-6109 01-073-3459 00-056-0556 04-007-1060 04-012-1725	SiO_2 $K_2Si_2O_5$ Fe_3O_4 K_2O KOH FeO	(slag) (s) (ss) (slag) (g) (slag)	Porous rock-hard black cake. Green traces on surface

4.1.1. Phase Composition

The binary system Fe_2O_3-SiO_2 did not show any signs of agglomeration or changes in physical characteristics. For the binary system Fe_2O_3-$CaCO_3$ some colour differences could be detected, including yellow and/or brown spots. As clear from Table 4, there were limited chemical transformations in both binary systems, but the compound $Ca_2Fe_2O_5$ was detected by XRD, which has a yellow-brown appearance [66]. The yellow spots found in these cases could be explained by this finding.

For the binary system Fe_2O_3-K_2CO_3 $KFeO_2$ was detected by XRD in both oxidising and reducing environments as indicated in *Table 4*. Both samples were difficult to extract from the ceramic boat and larger lumps were formed. These lumps indicate formation of clusters which include compounds from both ash and oxygen carrier components and clearly leads to agglomeration, characterised by a rock-hard structure. For the two ternary systems Fe_2O_3-$CaCO_3$-SiO_2 and Fe_2O_3-K_2CO_3-SiO_2 *Table 4* shows oxygen carrier-ash interactions. For Fe_2O_3-$CaCO_3$-SiO_2, similar to the binary system, $Ca_2Fe_2O_5$ was once again present. This can be confirmed visually once again with the observed yellow spots on the resulting material.

Figure 3 shows three photographs of the ternary system Fe_2O_3-K_2CO_3-SiO_2 before (left) and after (middle and right) exposure. These photographs were chosen as an example to illustrate the general characteristics of the samples before and after exposure. The samples were extracted from the ceramic boat and lightly crushed before photographed. It is clear from these images, that there were major changes in particle appearance during exposure.

Figure 3 Photos of ternary system Fe_2O_3- K_2CO_3-SiO_2 before (left) and after reducing (middle) and oxidising (right) exposure.

The highest degree of interactions was seen for the ternary Fe_2O_3-K_2CO_3-SiO_2 system. In contrast to the binary systems Fe_2O_3-K_2CO_3 and Fe_2O_3-SiO_2 iron was found to interact with silicon to form Fe-Si compounds after reducing exposure while Fe-K compounds were detected after oxidising exposure. In Figure 3 (middle) green traces are observed across the sample, which were not detected for the binary system Fe_2O_3-K_2CO_3. Fayalite compounds such as $Fe_{2.57}Si_{0.43}O_4$ and $Fe_{2.45}Si_{0.55}O_4$, have a greenish yellow or yellow-brown colour. The same colour can be observed in Figure 3 (right) confirming the presence of these compounds [66]. However, $Fe_xSi_yO_z$ compounds are not found during exposure with only silica. It is possible that the presence of potassium results in favourable conditions for forming these compounds.

4.1.2. Thermodynamic Predictions

The thermodynamic calculations assume thermodynamic equilibrium in the investigated systems, which may not always be the case. Therefore, one may experimentally observe unreacted compounds such as CaO and Fe_2O_3, while thermodynamically all the iron may interact to form $Ca_2Fe_2O_5$ and $CaFe_2O_4$ as seen in Table 4.

Characterisation of samples after exposure using XRD found that, with an exception for the binary system Fe_2O_3-SiO_2, some phase interactions took place during the experiments for all systems. Thermodynamic calculations did predict the outcome for the binary systems Fe_2O_3-$CaCO_3$ and Fe_2O_3-SiO_2 well. However, it did not predict formation of $KFeO_2$ for the Fe_2O_3-K_2CO_3 system due to lack of information in the databases. It was also found that potassium formed gaseous compounds such as K, KOH, $(KOH)_2$ and KO. It is therefore possible that these gaseous compounds interacted with hematite while diffusing to the surface of the ceramic boat.

4.2. Hausmannite

Table 5 presents thermodynamic calculations together with results from XRD analysis for hausmannite and ash experiments. In addition, the last column in the table provides information regarding the visual appearance of the product.

Table 5 Summarised results for exposures carried out with hausmannite.

Ash component		**XRD**		**FactSage**		**Visual**
		Compound	**PDF No**			
$CaCO_3$	Oxidising	***$CaMn_2O_4$*** CaO ***$CaMnO_3$*** Mn_3O_4	04-015-3975 04-002-6758 00-003-0830 04-007-1841	Mn_3O_4 CaO MnO	(ss1) (ss2) (ss2)	Soft and dark cake
$CaCO_3$	Reducing	***$CaMnO_3$*** ***$(MnO)_{0.614}(CaO)_{0.386}$*** ***$(MnO)_{0.253}(CaO)_{0.747}$*** MnO CaO	04-007-8030 01-077-2372 01-077-2374 04-005-4310 01-077-2370	MnO CaO	(ss1) (ss1)	Soft green cake
K_2CO_3	Oxidising	***K_2MnO_4*** Mn_3O_4 MnO_2	04-010-3595 03-065-2776 00-053-0633	Mn_3O_4 K_2O_2 K KO	(ss1) (s) (g) (g)	Porous, hard and dark cake
K_2CO_3	Reducing	K_2CO_3 ***K_3MnO_4*** MnO	00-056-0556 00-031-1050 04-005-4310	MnO KOH $(KOH)_2$ K Mn_2O_3	(ss1) (g) (g) (g) (ss1)	Porous, hard and dark cake. Green spots all over sample
SiO_2	Oxidising	Mn_3O_4 SiO_2	04-007-1841 00-046-1045	***Mn_7SiO_{12}*** SiO_2 Mn_8O_{12}	(ss1) (s) (ss1)	No visual change. Soft cake formed.
SiO_2	Reducing	MnO SiO_2	04-005-4310 01-089-1961	MnO ***Mn_2SiO_4*** Mn_2O_3	(ss1) (s) (ss1)	Green soft cake
$CaCO_3$ + SiO_2	Oxidising	***$CaMnO_3$*** SiO_2 CaO ***$CaMn_2O_4$*** Mn_3O_4	00-003-0830 00-061-0035 01-070-4068 04-015-3975 04-007-1841	Mn_3O_4 ***Mn_7SiO_{12}*** $Ca_3Si_2O_7$ Mn_8O_{12}	(ss1) (ss2) (s) (ss2)	Soft dark cake

	Reducing	***$CaMn_7O_{12}$*** MnO SiO_2 CaO	04-012-8184 04-005-4310 00-046-1045 01-077-7243	MnO ***$CaMnSiO_4$*** ***Mn_2SiO_4*** Ca_2SiO_4 CaO	(ss1) (ss2) (ss2) (ss2) (ss1)	Soft cake. Green spots all over sample
K_2CO_3 + SiO_2	Oxidising	Mn_3O_4 ***K_3MnO_4*** ***$K_2Mn_4O_8$*** ***$MnSiO_3$*** SiO_2	04-007-1841 00-031-1049 00-016-0205 04-012-8272 04-012-0813	Mn_3O_4 K_2SiO_3 SiO_2 K_2O	(ss1) (s) (slag) (slag)	Porous, hard and dark cake
	Reducing	K_2CO_3 MnO SiO_2	00-056-0556 04-005-4310 04-013-3639	MnO K_2SiO_3 SiO_2 K_2O KOH Mn_2O_3 K MnO $(KOH)_2$	(ss1) (s) (slag) (slag) (g) (ss1) (g) (slag) (g)	Porous, hard and dark cake. Green spots all over sample.

4.2.1. Phase Composition

The binary systems showed changes in both colour and physical characteristics of the samples during exposure. Some differences in both colour and consistency was detected depending on exposure environment. Three photos of Mn_3O_4-SiO_2 at different stages are shown in Figure 4 representing a mixture of hausmannite and silica before (left) and after reducing (middle) and oxidising (right) exposure. These photographs were chosen as an example to illustrate the general characteristics of the samples before and after exposure. It is clear from these images, that there were changes in colour during exposure, indicating some type of chemical transformation. Samples exposed in a reducing environment followed the same colour change and resulted either green spots or formation of a green cake, as clear from Figure 4. In each reducing environment the compound MnO is found, which has a green colour and could be the origin for this observation [66].

Figure 4 Photos of the binary system Mn_3O_4-SiO_2 before (left) and after and after reducing (middle) and oxidising (right) exposure.

Exposures for the binary systems Mn_3O_4-SiO_2 and Mn_3O_4-$CaCO_3$ formed a soft cake after exposure which could easily be crushed, similar to those in Figure 4. This indicates a mild agglomerating behaviour. For Mn_3O_4-SiO_2 no complexes could be found between manganese and silicon, however for Mn_3O_4-$CaCO_3$ compounds such as $CaMnO_3$ and $CaMn_2O_4$ were detected by XRD, evident from Table 5. For the binary system Mn_3O_4-K_2CO_3 K_2MnO_4 was observed after oxidising exposure and K_3MnO_4 after reducing exposure. Additionally, for the cases involving potassium, the compound K_2MnO_4 has a dark green appearance which may contribute to colour variations [66].

For the ternary Mn_3O_4-K_2CO_3-SiO_2 samples formed a porous hard cake. In conformity between these systems interacted compounds such as K_xMnO_y were detected by XRD, indicating formation of clusters including compounds from both ash and oxygen carrier components; which could explain similar appearance and agglomerating behaviour.

For the ternary system Mn_3O_4-$CaCO_3$-SiO_2; the interacted compound $CaMn_xO_y$ is formed in both environments, as evident from Table 5. This table also shows that the system Mn_3O_4-K_2CO_3-SiO_2 result in interaction between manganese and silicon, which form $MnSiO_3$, but also K_2MnO_4 and $K_2Mn_4O_8$. It is possible that the presence of potassium facilitated the interaction between the Mn_3O_4 and silica, in a similar way which was seen with Fe together with K and Si above.

4.2.2. Thermodynamic Predictions

As evident from Table 5, the correlation between experiments and thermodynamic predictions was poor. For the binary systems, manganese reacted with potassium and calcium, while no interaction was predicted. On the other hand, silica had limited interaction with the oxygen carrier, while a mixed Mn-Si oxide was predicted. Only for the ternary system of Mn_3O_4-$CaCO_3$-SiO_2 was $MnSiO_3$ formed.

In Table 5 the compounds $CaMn_2O_4$, $CaMnO_3$, K_3MnO_4, K_2MnO_4 and $K_2Mn_4O_8$ are found by XRD while the lack of data in FToxid results in no prediction of these compounds in the calculations.

4.3. Synthesised Ilmenite

Table 6 presents thermodynamic calculations together with results from XRD for synthesised ilmenite and ash experiments. In addition, the last column provides some information regarding the visual appearance of the product.

Table 6. Summarised results for exposures carried out with synthesised ilmenite.

Ash component		XRD		FactSage		Visual
		Compound	PDF No			
$CaCO_3$	Oxidising	Fe_2TiO_5 TiO_2 CaO	00-041-1432 04-003-0648 00-037-1497	***$CaTiO_3$*** Fe_2O_3	(s) (ss1)	Soft grey powder. Some darker grey areas
	Reducing	$FeTiO_3$ CaO	04-007-2813 01-070-4068	***$CaTiO_3$*** Fe_3O_4 $FeTi_2O_4$	(s) (ss1) (ss1)	Soft and yellow-brown powder

				Fe_3O_4	(ss2)	
K_2CO_3	Oxidising	$\boldsymbol{K_{0.85}Fe_{0.85}Ti_{0.15}O_2}$ $\boldsymbol{K_{0.4}Fe_{0.4}Ti_{0.6}O_2}$ $\boldsymbol{KFeO_2}$ $\boldsymbol{K_2Ti_2O_5}$	00-062-0213 04-010-9012 04-013-8446 04-012-6258	Fe_2O_3 $\mathbf{K_2Ti_3O_7}$ K_2O TiO_2 Fe_2O_3 FeO	(ss1) (s) (slag) (slag) (slag) (slag)	Black hard porous cake. Red-brown shades with yellow areas inside
	Reducing	$\boldsymbol{K_{0.85}Fe_{0.85}Ti_{0.15}O_2}$ $\boldsymbol{K_{0.4}Fe_{0.4}Ti_{0.6}O_2}$ $\boldsymbol{KFeO_2}$ Fe_3O_4	00-062-0213 04-010-9012 04-013-8446 04-012-7038	K_2O TiO_2 $FeTi_2O_4$ Fe_3O_4 FeO $\mathbf{K_2Ti_3O_7}$ KOH Fe_2O_3 K $FeTi_2O_4$ $(KOH)_2$ Ti_2O_3	(slag) (slag) (ss1) (ss1) (slag) (s) (g) (slag) (g) (ss1) (g) (slag)	Black hard porous cake with yellow areas on the surface.
SiO_2	Oxidising	Fe_2TiO_5 TiO_2 SiO_2	04-015-5398 04-003-0648 01-089-1961	TiO_2 Fe_2O_3 SiO_2 Ti_2O_3	(ss1) (ss2) (s) (ss1)	Slightly brighter grey shade
	Reducing	$FeTiO_3$ SiO_2	04-007-2813 00-046-1045	$FeTiO_3$ SiO_2 Ti_2O_3 Fe_3O_4 $FeTi_2O_4$	(ss1) (s) (ss1) (ss2) (ss2)	Slightly darker grey shade
$CaCO_3$ + SiO_2	Oxidising	Fe_2TiO_5 CaO TiO_2 SiO_2	04-015-5398 01-070-4068 04-003-0648 01-089-1961	$\boldsymbol{CaSiTiO_5}$ Fe_2O_3 TiO_2 Ti_2O_3 Ti_2O_3	(s) (ss1) (ss2) (ss1) (ss2)	Soft grey powder. Some darker areas.
	Reducing	$FeTiO_3$ CaO SiO_2	04-007-2813 01-070-4068 00-046-1045	$\boldsymbol{CaSiTiO_5}$ Fe_3O_4 $FeTi_2O_4$ $CaSiO_3$ $FeTi_2O_4$ $CaTiO_3$	(s) (ss1) (ss1) (ss2) (ss1) (s)	Soft dark yellow-brown powder
K_2CO_3 + SiO_2	Oxidising	$\boldsymbol{K_{0.4}Fe_{0.4}Ti_{0.6}O_2}$ Fe_2TiO_5	04-010-9012 04-015-5398	TiO_2 Fe_2O_3	(slag) (ss1)	Black rock-hard porous cake with.

		SiO_2 ***$K_{0.012}Ti_8O_{16}$*** K_4SiO_4	00-046-1045 01-081-2039 04-010-7078	TiO_2 K_2O SiO_2 $K_2Si_2O_5$ Fe_2O_3 FeO	(ss2) (slag) (slag) (s) (slag) (slag)	Red-brown shades with yellow spots inside the cake
	Reducing	***$K_{0.4}Fe_{0.4}Ti_{0.6}O_2$*** $FeTiO_3$ Fe_2TiO_4 K_4SiO_4	04-010-9012 00-029-0733 00-034-0177 04-010-7078	TiO_2 K_2O SiO_2 $FeTi_2O_4$ Fe_3O_4 $K_2Si_2O_5$ $FeTiO_3$ KOH FeO $FeTi_2O_4$ K	(slag) (slag) (slag) (ss1) (ss1) (s) (ss2) (g) (slag) (ss1) (g)	Black rock-hard porous cake with yellow areas on the surface. Denser inside.

4.3.1. Phase Composition

The behaviour of ilmenite during exposure is similar to the results above, where potassium showed the highest driving force for reaction with ilmenite. The binary system $FeTiO_3$-K_2CO_3 formed a rock-hard cake, and mostly interacted compounds are detected. Similar to the system in Table 4, for Fe_2O_3-K_2CO_3 and Fe_2O_3-K_2CO_3-SiO_2, yellow and red-brown areas could be found for both $FeTiO_3$-K_2CO_3 and $FeTiO_3$-K_2CO_3-SiO_2. One possibility for these yellow spots could be the formation of K_2O which has a pale-yellow colour. The red-brown tone could be a result from the compound $KFeO_2$ detected with XRD [66].

In contrast to the binary system $FeTiO_3$-K_2CO_3, the systems $FeTiO_3$-SiO_2 and $FeTiO_3$-$CaCO_3$ showed no changes in physical characteristics or agglomeration except some mild colour changes. This is further verified by XRD which did not find any interaction between ilmenite and ash component. XRD indicates that the oxygen carrier is found in its oxidised form (Fe_2TiO_5 + TiO_2) and reduced form ($FeTiO_3$) in respective environment for each exposure.

For the ternary system $FeTiO_3$-$CaCO_3$-SiO_2 no interacted compounds were detected, and the visual appearance was similar to the binary system. As an example, three photos are presented in Figure 5 to illustrate the physical properties of synthesised ilmenite with calcium carbonate and silica. The same properties were observed for the binary system $FeTiO_3$-$CaCO_3$.

Figure 5 Photos of the ternary system $FeTiO_3$-$CaCO_3$-SiO_2 before (left) and after oxidising (middle) and reducing (right) exposure.

In the case of the ternary system $FeTiO_3$-K_2CO_3-SiO_2, the oxygen carrier interacted with potassium forming $K_xFe_yTi_zO_w$ just as in the binary case $FeTiO_3$-K_2CO_3. However, interaction was also found between the ash components, forming K_4SiO_4. It is possible that potassium formed gaseous compounds such as KOH which thereafter interacted with silica. The formation of gaseous potassium compounds is also indicated in thermodynamic calculations. The shape of the diffractogram for the ternary system $FeTiO_3$-K_2CO_3-SiO_2 for both environments consisted of diffuse peaks with low intensities, indicating presence of amorphous phases, possibly due to interaction between potassium and silica.

4.3.2. Thermodynamic Predictions

The binary system $FeTiO_3$-SiO_2 was well predicted by the thermodynamical calculations. There were no interacted compounds between oxygen carrier and ash component predicted nor detected. On the other hand, calculations for the binary system $FeTiO_3$-$CaCO_3$ predicted $CaTiO_3$ while visual and XRD results showed no indication of interaction. There were some colour changes during experiments, but this could be due to intrinsic phase changes of the oxygen carrier, or initial transformation during heating.

For the binary system $FeTiO_3$-K_2CO_3, calculations predicted $K_2Ti_3O_7$ and a slag phase to be formed in both environments. The diffractogram from the physical experiments consisted of relatively clear high intensity peaks, with a few exceptions of broader peaks. XRD found $K_xFe_yTi_zO_w$ compounds in both environments. However, $K_xFe_yTi_zO_w$-compounds are not included in FactSage and prediction of these is not possible.

For the ternary system $FeTiO_3$-K_2CO_3-SiO_2 thermodynamics showed a complex outcome with gaseous and slag phases. These calculations predicted interaction between ash components $K_2Si_2O_5$, while XRD found K_4SiO_4. Similar to the binary system, formation of $K_xFe_yTi_zO_w$- and $K_xTi_yO_z$-compounds failed to be predicted. However, the diffractogram of ternary system was diffuse and difficult to analyse due to broad peaks with low intensities. This indicates that the slag phase could have contributed to formation of amorphous phases. Agglomeration induced by the high temperature may be one explanation for the results including potassium and silica. Former studies show that reaction between silica and potassium occur in solid-solid phase at temperatures around 700℃ [18]. Since the exposure temperature was 900℃ this may be a possibility, also indicated by the formation of K_4SiO_4.

5. Discussion

When utilising biomass in CLC and OCAC different forms of biomass could be considered, meaning that impurities and trace elements could be present in varying, but sometimes high concentrations [44]. This study investigates different environments, ash components and oxygen carriers for the CLC and OCAC processes. In a real system, oxygen carriers will be fluidised, exposed to different environments, endure different gradients of temperature and high velocities. By utilising fixed bed conditions, more contact and an extensive time of contact is achieved compared to a fluidised bed.

The reaction paths for the ash compounds may vary considerably and be composed of several steps. Some compounds may interact with the oxygen carrier after evaporating or interacting with another compound. This may be especially interesting for the experiments including alkali, where pure and gas phases could be present, together with slag phases. In addition to the components investigated in this work biomass fuels may contain various amount of chlorine and nitrates. Potassium forms perchlorates/nitrates at lower temperatures (100-250°C), which thereafter decomposes and melts (200-700°C) while releasing Cl/N [44]. These compounds may thereafter interact with the bed material either in gaseous or solid form, which in that case will not be in the form of carbonates, as used in these experiments. However, by using solid carbonate and silicate compounds the reaction mechanism is simplified and one aspect of the possible interaction is investigated. Furthermore, ash concentrations in a real CLC processes are generally lower compared to the 1:1 and 1:0.5:0.5 molar ratio [67]. How the oxygen carrier react in fluidised bed may be very different in comparison to the mechanism whereby they react in this study. Still, the long exposure time and enhanced contact should provide some type of worst-case scenario and give indication of possible phases which could be formed in the current environment.

The binary systems including potassium showed to form either gas- or slag phases, or both. Since pores were detected in all samples involving potassium and gaseous compounds were predicted by thermodynamic calculations it is a clear indication that some potassium has entered gas phase. Thus, it is possible that potassium melted during exposure making the oxygen carriers more prone to form amorphous compounds which could induce agglomeration. The melting point of potassium carbonate is 899°C [68]. Therefore, it is likely that potassium melted during exposure making the oxygen carriers more prone to deform, but also promote intraparticle diffusion. The observed porosity could also be due to evaporation of potassium during reaction. Thermodynamics showed that the gas phase included KOH, KO, K and/or $(KOH)_2$.

One possibility for ternary systems when increasing the temperature beyond 700°C is that potassium silicates convert to molten slag phase. The formation of a slag phase could have facilitated diffusion of potassium and silicon into the particles. Also, depending on the ratio between potassium and silicon different compounds can be found, for example K_2SiO_3 or $K_2Si_2O_5$ [18]. It is possible that slight differences in composition is present during exposure in different areas of the ceramic boat. This is consistent with literature where one mechanism for coating formation is when silicon interacts with gaseous potassium to form a sticky compound which could in its turn form a layer on the bed material [45]. Since there is a relatively high amount of ash in these experiments there could be enough molten phase present to form agglomerates. This could also be noted in the visual inspection where rock-hard cakes were formed.

Ash components that stick to the surface could affect the particle in several ways. These components may diffuse into the particles resulting in volume expansion and cracks. Reaction may occur after diffusion where for example the carbonate or ash component leaves with the gas phase. Lastly, reaction may occur on the surface, before diffusion, which leads to cracks and holes in the oxygen carrier particles. This may also explain the porous samples of hematite and hausmannite when exposed with potassium. Hausmannite and hematite showed to interact to a higher extent compared with synthesised ilmenite regarding both visual inspection and detectable phases. The particle size for silica and potassium carbonate are smaller compared to calcium carbonate. This could influence the reaction mechanism which allows for the smaller ash components to diffuse into the particles. However, it is believed that the holding time is sufficient to initiate reactions between the components and it is clear from the analysis that all components reacted in some systems, although equilibrium may not have been obtained. Previous studies have examined ilmenite as oxygen-carrying bed material for OCAC in a 12 MW_{th} CFB boiler with biomass as fuel. Samples which have been in the system for only one hour showed accumulation of calcium on the surface layer [60]. The study also showed that after 24 h a calcium-rich double layer could be identified [60]. Thus, due to the six hours exposure time in this paper, the initial mechanism of the formation of one surface layer can be expected to occur.

Some words should be said regarding the thermodynamic calculations and comparison to the experimental results. For the binary systems including calcium and silicon the thermodynamic calculations predicted the outcome well. The binary systems including potassium did not provide the same degree of correspondence. When including potassium into these systems some uncertainties can be expected since databases including potassium are not complete.

Amongst the oxygen carriers hausmannite was shown to give the least consistent thermodynamic results. Systems including manganese have not been optimised which has resulted in some mismatching predictions, as indicated in *Table 5*. In FactSage, the database FToxid includes systems containing CoO, NiO, ZnO, PbO, MnO and Mn_2O_3 with major oxide components Al_2O_3, CaO, FeO, Fe_2O_3, MgO, SiO_2. Many ternary and most binary sub-systems among these components and between these components and the major oxide components have been evaluated and optimised. However, the systems involving MnO and Mn_2O_3 are an exception [69]. Optimisations and evaluations have only been performed for the system MnO-Mn_2O_3-FeO-Fe_2O_3-SiO_2, which might explain why compounds including manganese and silicon are formed but not manganese and calcium [69]. These systems may not cover all composition ranges and are therefore assumed ideal or approximated. For example, addition of Na_2O and K_2O to the previously mentioned major system will result in some uncertainties [69, 70]. The following compounds were identified to be missing in the databases $K_xFe_yO_z$, $K_xFe_yTi_zO_w$, $K_xTi_yO_z$, $K_xMn_yO_z$ and $CaMn_xO_y$. Possibly the main reason why these combinations show the most diverse results.

Some of the differences could also be because high activation energies of reactions and meaning that certain kinetically controlled transformations are neglected in the calculations [54]. Based on this, it is also difficult to determine whether these reactions will occur during the experimental period of six hours. It is possible that a longer exposure time would result in more consistency between thermodynamic and experimental results. On the other hand, longer exposure times would make the conditions even less relevant for the conditions in large scale operation.

Due to the XRD limitations, crystalline compounds below five mass percent and amorphous compounds cannot be detected, which may limit the suitability of the characterisation process [71]. It is known that potassium has a tendency to form amorphous compounds [72]. These types of compounds do not have a defined lattice pattern, resulting in scattering of the x-rays in many directions. Broader peaks with lower intensities could indicate presence of these amorphous compounds. For instance, the compound K_4SiO_4 was detected by XRD for the ternary system $FeTiO_3$-K_2CO_3-SiO_2 after reducing exposure. The presence of this compound indicates interaction between the ash components potassium and silicon. Thermodynamic calculations on the other hand predicted K_2SiO_3 and $K_2Si_2O_5$. These were not detected by XRD, since they are amorphous [66]. Therefore, their presence cannot be excluded. This pattern was only observed in the ternary systems including the ash components K_2CO_3 and SiO_2. The same observation was made for the two ternary systems Fe_2O_3-K_2CO_3-SiO_2 and Mn_3O_4-K_2CO_3-SiO_2.

Another factor is that the thermodynamical calculations are performed at 900°C while the samples are cooled down to room temperature before analysed with XRD. The cooling process was simulated in FactSage by using the resulting phases as input and then simulating a cool-down to 25°C. The calculation predicted the same phases and therefore the cooldown is assumed to have a negligible effect on the result.

It is clear from the experiments in this study, that common ash components can interact with the oxygen carrier and that binary and ternary systems do not demonstrate the same behaviour. The study showed similar outcome regarding interaction for calcium and silicon, however the reaction path of potassium is much more complex with interaction seen for all investigated systems, often forming hard agglomerates during both oxidizing and reducing conditions.

Synthesised ilmenite only formed new compounds in the case with potassium. Hematite and hausmannite interacted with calcium forming $Ca_2Fe_2O_5$ and $Ca_xMn_yO_z$ in both the binary and ternary system. These samples did not form hard agglomerates even though slight consistency change was observed. Based on the degree of interaction, synthesised ilmenite is shown to be most stable oxygen carrier in this study.

6. Conclusions

Chemical-looping could be an interesting technology for converting biomass or bio-waste. However, the high fractions of reactive ash components may have implications for the oxygen carrier, which needs to have a high functionality and transportability. Fixed bed experiments performed in this study showed that some common iron and manganese-based oxygen carriers and ash species react to different extents. Hausmannite and hematite showed to interact to a higher extent compared with synthesised ilmenite regarding both visual inspection and detectable phases. The main conclusions of the study are;

- Binary systems with silica did not result in any interaction with the oxygen carriers.
- Hematite and hausmannite formed $Ca_2Fe_2O_5$ and $Ca_xMn_yO_z$ in both binary and ternary systems while no interaction was noticed for ilmenite. There was no sign of agglomeration in either case.
- Binary systems with K_2CO_3 and ternary systems with K_2CO_3 and SiO_2 formed new phases which were accompanied by severe agglomeration.
- Synthesised ilmenite showed the least degree of interaction.
- Results from thermodynamic calculations agreed relatively well for both binary and ternary systems with the oxygen carrier ilmenite and hematite and ash components calcium and silicon. Lack of thermodynamic data is likely the main reason for non-consistent result for systems including potassium and manganese. Following compounds were identified to be missing in the databases; $K_xFe_yO_z$, $K_xFe_yTi_zO_w$, $K_xTi_yO_z$, $K_xMn_yO_z$ and $CaMn_xO_y$. This suggests that thermodynamic optimisation of systems involving manganese and/or potassium should be performed.

Acknowledgement

The authors acknowledge the work of the late Dongmei Zhao (deceased Dec 18, 2016). At the time of her death, she was closely involved with this research and made many important contributions. This work was financed by Formas, the Swedish Research Council for Environment, Agricultural Sciences and Spatial Planning (2017-01095) and the Swedish Research Council (VR project number 2016-06023).

References

[1] IPCC. Climate Change 2013 The Physical Science Basis Working Group I Contribution to the Fifth Assessment Report of the Intergovernmental Panel on Climate Change. In: Stocker T, Qin D, Plattner G, Tignor M, Allen S, Boschung J, et al., editors. Cambridge, United Kingdom and New York, USA2013.
[2] IPCC. Climate Change 2014: Mitigation of Climate Change. Contribution of Working Group III to the Fifth Assessment Report of the Intergovernmental Panel on Climate Change. In: Edenhofer O, Pichs-Madruga R, Sokona Y, Farahani E, Kadner S, Seyboth K, et al., editors. Cambridge, United Kingdom and New York, USA2014.
[3] IPCC. Summary for Policymakers. In: Global warming of 1.5°C. An IPCC Special Report on the impacts of global warming of 1.5°C above pre-industrial levels and related global greenhouse gas emission pathways, in the context of strengthening the global response to the threat of climate change, sustainable development, and efforts to eradicate poverty. In: V. Masson-Delmotte, P. Zhai, H. O. Pörtner, D. Roberts, J. Skea, P. R. Shukla, et al., editors. Geneva, Switzerland.2018. p. 32 pp.
[4] IPCC. IPCC Special Report on Carbon Dioxide Capture and Storage. In: Metz B, Davidson O, de Coninck H, Loos M, Meyer L, editors. Cambridge, United Kingdom2005.
[5] Gasser T, Guivarch C, Tachiiri K, Jones CD, Ciais P. Negative emissions physically needed to keep global warming below 2°C. Nature Communications. 2015;6.
[6] Azar C, Lindgren K, Obersteiner M, Riahi K, van Vuuren DP, den Elzen KMGJ, et al. The feasibility of low CO2 concentration targets and the role of bio-energy with carbon capture and storage (BECCS). Climatic Change. 2010;100:195-202.
[7] Lyngfelt A, Leckner B, Mattisson T. A fluidized-bed combustion process with inherent CO2 separation; application of chemical-looping combustion. Chemical Engineering Science. 2001;56:3101-13.
[8] Adanez J, Abad A, Garcia-Labiano F, Gayan P, de Diego LF. Progress in Chemical-Looping Combustion and Reforming technologies. Progress in Energy and Combustion Science. 2012;38:215-82.
[9] Boot-Handford ME, Abanades JC, Anthony EJ, Blunt MJ, Brandani S, Mac Dowell N, et al. Carbon capture and storage update. Energy and Environmental Science. 2014;7:130-89.
[10] Lyngfelt A. Oxygen carriers for chemical-looping combustion. In: Fennell P, Anthony B, editors. Calcium and Chemical Looping Technology for Power Generation and Carbon Dioxide (CO2) Capture. 1st ed: Woodhead Publishing; 2015. p. 221-54.
[11] Adánez J, Abad A, Mendiara T, Gayán P, de Diego LF, García-Labiano F. Chemical looping combustion of solid fuels. Progress in Energy and Combustion Science. 2018;65:6-66.
[12] Ohlemüller P, Ströhle J, Epple B. Chemical looping combustion of hard coal and torrefied biomass in a 1 MWth pilot plant. International Journal of Greenhouse Gas Control. 2017;65:149-59.
[13] Schmitz M, Linderholm C. Chemical looping combustion of biomass in 10- and 100-kW pilots – Analysis of conversion and lifetime using a sintered manganese ore. Fuel. 2018;231:73-84.
[14] Thunman H, Lind F, Breitholtz C, Berguerand N, Seemann M. Using an oxygen-carrier as bed material for combustion of biomass in a 12-MWth circulating fluidized-bed boiler. Fuel. 2013;113:300-9.
[15] Hanning M, Gyllén A, Lind F, Rydén M. Biomass ash interactions with a manganese ore used as oxygen-carrying bed material in a 12 MWth CFB boiler. Biomass and Bioenergy. 2018;119:179-90.
[16] Wang P, Leion H, Yang HR. Oxygen-Carrier-Aided Combustion in a Bench-Scale Fluidized Bed. Energy and Fuels. 2017;31:6463-647.

[17] Lind F, Corcoran A, Andersson B, Thunman H. 12,000 Hours of Operation with Oxygen-Carriers in Industrially Relevant Scale (75,000 kWth). VGB PowerTech. 2017.
[18] Anicic B, Lin W, Dam-Johansen K, Wu H. Agglomeration mechanism in biomass fluidized bed combustion – Reaction between potassium carbonate and silica sand. Fuel Processing Technology. 2018;173:182-90.
[19] Morris JD, Daood SS, Chilton S, Nimmo W. Mechanisms and mitigation of agglomeration during fluidized bed combustion of biomass: A review. Fuel. 2018;230:452-73.
[20] Grimm A, Skoglund N, Boström D, Öhman M. Bed agglomeration characteristics in fluidized quartz bed combustion of phosphorus-rich biomass fuels. Energy & Fuels. 2011;25:937-47.
[21] Grimm A, Öhman M, Lindberg T, Fredriksson A, Boström D. Bed agglomeration characteristics in fluidized-bed combustion of biomass fuels using olivine as bed material. Energy and Fuels. 2012;26:4550-9.
[22] Corcoran A, Knutsson P, Lind F, Thunman H. Mechanism for migration and layer growth of biomass ash on ilmenite used for oxygen carrier aided combustion. Energy and Fuels. 2018.
[23] Gu H, Shen L, Zhong Z, Zhou Y, Liu W, Niu X, et al. Interaction between biomass ash and iron ore oxygen carrier during chemical looping combustion. Chemical Engineering Journal. 2015;277:70-8.
[24] Lyngfelt A. Chemical-looping combustion of solid fuels - Status of development. Appl Energy. 2014;113:1869-73.
[25] Mattisson T, Lyngfelt A, Leion H. Chemical-looping with oxygen uncoupling for combustion of solid fuels. International Journal of Greenhouse Gas Control. 2009;3:11-9.
[26] Dong C, Jiang J, Yang Y, Zhang J, Shan L. Research on the reactivity of oxygen carrier Fe2O3 for chemical looping combustion (CLC). Asia-Pacific Power and Energy Engineering Conference, APPEEC2010.
[27] Jerndal E, Mattisson T, Lyngfelt A. Thermal Analysis of Chemical-Looping Combustion. Chemical Engineering Research and Design. 2006;84:795-806.
[28] Abad A, Adánez J, García-Labiano F, de Diego LF, Gayán P, Celaya J. Mapping of the range of operational conditions for Cu-, Fe-, and Ni-based oxygen carriers in chemical-looping combustion. Chemical Engineering Science. 2007;62:533-49.
[29] Mendiara T, Abad A, de Diego LF, García-Labiano F, Gayán P, Adánez J. Biomass combustion in a CLC system using an iron ore as an oxygen carrier. International Journal of Greenhouse Gas Control. 2013;19:322-30.
[30] Linderholm C, Schmitz M. Chemical-looping combustion of solid fuels in a 100 kW dual circulating fluidized bed system using iron ore as oxygen carrier. Journal of Environmental Chemical Engineering. 2016;4:1029-39.
[31] Knutsson P, Linderholm C. Characterization of ilmenite used as oxygen carrier in a 100 kW chemical-looping combustor for solid fuels. Appl Energy. 2015;157:368-73.
[32] Cuadrat A, Abad A, García-Labiano F, Gayán P, de Diego LF, Adánez J. The use of ilmenite as oxygen-carrier in a 500Wth Chemical-Looping Coal Combustion unit. International Journal of Greenhouse Gas Control. 2011;5:1630-42.
[33] Moldenhauer P, Rydén M, Mattisson T, Younes M, Lyngfelt A. The use of ilmenite as oxygen carrier with kerosene in a 300 W CLC laboratory reactor with continuous circulation. Appl Energy. 2014;113:1846-54.
[34] Liu F, Zhang Y, Chen L, Qian D, Neathery JK, Kozo S, et al. Investigation of a Canadian ilmenite as an oxygen carrier for chemical looping combustion. Energy and Fuels. 2013;27:5987-95.

[35] Liang ZY, Dong CQ, Qin W, Lin CF. Review on optimization of iron based oxygen carriers in chemical-looping combustion. Xiandai Huagong/Modern Chemical Industry. 2017;37:36-40.
[36] Abad A, Mattisson T, Lyngfelt A, Rydén M. Chemical-looping combustion in a 300 W continuously operating reactor system using a manganese-based oxygen carrier. Fuel. 2006;85:1174-85.
[37] Xu L, Sun H, Li Z, Cai N. Experimental study of copper modified manganese ores as oxygen carriers in a dual fluidized bed reactor. Appl Energy. 2016;162:940-7.
[38] Moldenhauer P, Sundqvist S, Mattisson T, Linderholm C. Chemical-looping combustion of synthetic biomass-volatiles with manganese-ore oxygen carriers. International Journal of Greenhouse Gas Control. 2018;71:239-52.
[39] Schmitz M, Linderholm C, Hallberg P, Sundqvist S, Lyngfelt A. Chemical-Looping Combustion of Solid Fuels Using Manganese Ores as Oxygen Carriers. Energy and Fuels. 2016;30:1204-16.
[40] Linderholm C, Schmitz M, Knutsson P, Lyngfelt A. Chemical-looping combustion in a 100-kW unit using a mixture of ilmenite and manganese ore as oxygen carrier. Fuel. 2016;166:533-42.
[41] Linderholm C, Schmitz M, Biermann M, Hanning M, Lyngfelt A. Chemical-looping combustion of solid fuel in a 100 kW unit using sintered manganese ore as oxygen carrier. International Journal of Greenhouse Gas Control. 2017;65:170-81.
[42] Arjmand M, Leion H, Mattisson T, Lyngfelt A. Investigation of different manganese ores as oxygen carriers in chemical-looping combustion (CLC) for solid fuels. Appl Energy. 2014;113:1883-94.
[43] James AK, Thring RW, Helle S, Ghuman HS. Ash management review-applications of biomass bottom ash. Energies. 2012;5:3856-73.
[44] Vassilev SV, Baxter D, Vassileva CG. An overview of the behaviour of biomass during combustion: Part I. Phase-mineral transformations of organic and inorganic matter. Fuel. 2013;112:391-449.
[45] Zevenhoven M, Yrjas P, Hupa M. Ash-forming matter and ash-related problems New York: Wiley and Sons; 2010.
[46] Hupa M. Ash-related issues in fluidized-bed combustion of biomasses: Recent research highlights. Energy and Fuels. 2012;26:4-14.
[47] Khan AA, de Jong W, Jansens PJ, Spliethoff H. Biomass combustion in fluidized bed boilers: Potential problems and remedies. Fuel Processing Technology. 2009;90:21-50.
[48] Niu Y, Tan H, Hui S. Ash-related issues during biomass combustion: Alkali-induced slagging, silicate melt-induced slagging (ash fusion), agglomeration, corrosion, ash utilization, and related countermeasures. Progress in Energy and Combustion Science. 2016;52:1-61.
[49] Rubel A, Zhang Y, Liu K, Neathery J. Effect of ash on Oxygen Carriers for the application of Chemical Looping Combustion. Oil and Gas Science and Technology. 2011;66:291-300.
[50] Siriwardane R, Tian H, Richards G, Simonyi T, Poston J. Chemical-looping combustion of coal with metal oxide oxygen carriers. Energy and Fuels. 2009;23:3885-92.
[51] Wang B, Yan R, Zhao H, Zheng Y, Liu Z, Zheng C. Investigation of chemical looping combustion of coal with CuFe 2O4 oxygen carrier. Energy and Fuels. 2011;25:3344-54.
[52] Azis MM, Leion H, Jerndal E, Steenari BM, Mattisson T, Lyngfelt A. The Effect of Bituminous and Lignite Ash on the Performance of Ilmenite as Oxygen Carrier in Chemical-Looping Combustion. Chemical Engineering and Technology. 2013;36:1460-8.

[53] Rubel A, Zhang Y, Neathery JK, Liu K. Comparative study of the effect of different coal fly ashes on the performance of oxygen carriers for chemical looping combustion. Energy and Fuels. 2012;26:3156-61.
[54] Keller M, Arjmand M, Leion H, Mattisson T. Interaction of mineral matter of coal with oxygen carriers in chemical-looping combustion (CLC). Chemical Engineering Research and Design. 2014;92:1753-70.
[55] Bao J, Li Z, Cai N. Interaction between iron-based oxygen carrier and four coal ashes during chemical looping combustion. Appl Energy. 2014;115:549-58.
[56] Schwebel GL, Leion H, Krumm W. Comparison of natural ilmenites as oxygen carriers in chemical-looping combustion and influence of water gas shift reaction on gas composition. Chemical Engineering Research and Design. 2012;90:1351-60.
[57] Ilyushechkin AY, Kochanek M, Lim S. Interactions between oxygen carriers used for chemical looping combustion and ash from brown coals. Fuel Processing Technology. 2016.
[58] Gong R, Qin C, He D, Tan L, Ran J. Oxygen Uncoupling of Cu-based Oxygen Carrier with the Presence of Coal Ash in Chemical Looping Process. Energy and Fuels. 2018;32:7708-17.
[59] Zhang S, Xiao R. Performance of iron ore oxygen carrier modified by biomass ashes in coal-fueled chemical looping combustion. Greenhouse Gases: Science and Technology. 2016;6:695-709.
[60] Corcoran A, Marinkovic J, Lind F, Thunman H, Knutsson P, Seemann M. Ash properties of ilmenite used as bed material for combustion of biomass in a circulating fluidized bed boiler. Energy and Fuels. 2014;28:7672-9.
[61] Zevenhoven M, Sevonius C, Salminen P, Lindberg D, Brink A, Yrjas P, et al. Defluidization of the oxygen carrier ilmenite – Laboratory experiments with potassium salts. Energy. 2018;148:930-40.
[62] Leion H, Mattisson T, Lyngfelt A. Use of ores and industrial products as oxygen carriers in chemical-looping combustion. Energy and Fuels. 2009;23:2307-15.
[63] Azis MM, Jerndal E, Leion H, Mattisson T, Lyngfelt A. On the evaluation of synthetic and natural ilmenite using syngas as fuel in chemical-looping combustion (CLC). Chemical Engineering Research and Design. 2010;88:1505-14.
[64] Stuer M, Zhao Z, Bowen P. Freeze granulation: Powder processing for transparent alumina applications. Journal of the European Ceramic Society. 2012;32:2899-908.
[65] Staničić I, Andersson V, Hanning M, Mattisson T, Backman R, Leion H. Combined manganese oxides as oxygen carriers for biomass combustion — Ash interactions. Chemical Engineering Research and Design. 2019;149:104-20.
[66] John W. Anthony, Richard A. Bideaux, Bladh KW, Monte C. Nichols. Eds., Handbook of Mineralogy, Mineralogical Society of America. Chantilly, VA 20151-1110, USA.2004.
[67] Biedermann F, Obernberger I. Ash-related Problems during Biomass Combustion and Possibilities for a Sustainable Ash Utilisation. Aberdeen: Elsevier Ltd; 2005. 2005.
[68] Lehman RL, Gentry JS, Glumac NG. Thermal stability of potassium carbonate near its melting point. Thermochim Acta. 1998;316:1-9.
[69] Bale CW, Bélisle E, Chartrand P, Decterov SA, Eriksson G, Gheribi AE, et al. FactSage Thermochemical Software and Databases - 2010 - 2016. Calphad. 2016;54:35-53.
[70] Bale CW, Bélisle E, Chartrand P, Decterov SA, Eriksson G, Hack K, et al. FactSage thermochemical software and databases — recent developments. CALPHAD. 2009;33:295-311.
[71] Newman JA, Schmitt PD, Toth SJ, Deng F, Zhang S, Simpson GJ. Parts per Million Powder X-ray Diffraction. Analytical Chemistry. 2015;87:10950-5.

[72] Zhang H, Li J, Yang X, Guo S, Zhan H, Zhang Y, et al. Influence of coal ash on potassium retention and ash melting characteristics during gasification of corn stalk coke. Bioresour Technol. 2018;270:416-21.